



Contents lists available at ScienceDirect

Physics Letters A

www.elsevier.com/locate/pla



Generalized Newtonian and Herschel–Bulkley yield stress fluids pressure behavior near the tip of a sharp edge in thin film flows

Laurent Chupin, Liviu Iulian Palade*

Université de Lyon, CNRS INSA-Lyon, Institut Camille Jordan UMR5208 & Pôle de Mathématiques, Bât. Léonard de Vinci No. 401, 21 avenue Jean Capelle, F-69621 Villeurbanne, France

ARTICLE INFO

Article history:

Received 16 May 2008

Received in revised form 18 July 2008

Accepted 27 August 2008

Available online 2 September 2008

Communicated by F. Porcelli

Keywords:

Symmetrical and antisymmetrical flows

around sharp edge

Power law fluid

Carreau–Yasuda fluid

Bingham and Herschel–Bulkley yield stress fluids

ABSTRACT

The Letter deals with two-dimensional symmetric and antisymmetric flows of generalized Newtonian and Herschel–Bulkley yield stress fluids close to a sharp edge which, for modeling purposes, is taken to be a geometric singularity. The pressure field is approximated using an asymptotic expansion valid in the tip neighborhood, and its dependence upon the edge angle is studied. For these special flows, the methodology used to obtain the pressure behavior does not require explicit knowledge of the viscosity dependence upon shear rate. Moreover, we prove that whenever the tip angle is such that the edge is hollow shaped, the yield stress fluid behaves solid-like in a neighborhood domain of the tip.

© 2008 Elsevier B.V. All rights reserved.

1. Introduction

Hele–Shaw flows are common to many industrial applications, e.g. thin film injection molding, flows of relevance to tribology, etc. Commonly, they refer to flows confined between two parallel plates that are close to each other. The free boundary of the fluid film may, on the one hand, take any closed shape, and on the other, encounter obstacles of different geometries (such as sharp edges) placed perpendicular to the direction of flow. The early Hele–Shaw studies focused on Newtonian fluids. Moffatt [1] studied the flow behavior near a sharp corner confined between two intersecting, fixed plane surfaces and found the presence of eddies only for angles between rigid planes less than a critical value, and their absence for free surface flows. Hieber and Shen [2] carried out numerical simulations of Hele–Shaw filling flow of a thin planar cavity by a power law fluid and focused on tracking down the advancing fluid front. Later, Hassager and Lauridsen [3] focused on Hele–Shaw flows of a power law fluid around sharp corners, while Huilgol and Tanner [4] have presented an approximate solution to the problem of a second order fluid leaving a straight edge. More recently, Aronsson and Janfalk [5] carried out a rigorous mathematical analysis of the pressure behavior of a power law fluid around a sharp edge. However, for more complex viscosity

laws—such as Bingham or Herschel–Bulkley fluids—modeling Hele–Shaw flows requires a different theoretical framework. That this is indeed the case may be reckoned from Huilgol's recent work [6], where the flow equations are obtained by making use of the viscometric fluidity function.

In this Letter we extend the analysis of Hele–Shaw flows around a sharp edge (the tip of which is assumed a geometric singularity) and present new results on the pressure dependence vs. edge angle for the following liquids:

- *Generalized Newtonian fluids*, in which case the results are obtained without specific reference to the explicit dependence of the viscosity upon the shear rate $\dot{\gamma}$. This has been achieved by generalizing the method given in [3] and [5], where only power law fluids were studied. Furthermore, we address the Carreau–Yasuda fluid issue as well.
- *Yield stress fluids*, for which the pressure pattern has never been studied before.

The Letter is organized as following. Section 2 contains a concise presentation of the general constitutive laws being used (for sake of clarity). The equations of thin film flow motion, which result in a simplified boundary value problem whose unique unknown is the pressure field, are given next. The way they are obtained is similar to that shown in [3] and [7]. In Section 3, we study the pressure behavior in a neighborhood of a sharp edge, in a system of polar coordinates centered at the edge tip. Next we present several theoretical results of relevance to the pressure be-

* Corresponding author.

E-mail addresses: laurent.chupin@insa-lyon.fr (L. Chupin), liviu-iulian.palade@insa-lyon.fr (L.I. Palade).

havior, valid for two particular flows: antisymmetric (perpendicular to the edge axis of symmetry) and symmetric (directed towards the edge and parallel to its axis of symmetry). In doing so, we assume that the pressure field in the neighborhood of $r = 0$ is of the form:

$$p(r, \theta) = r^m \varphi(\theta) + o(r^m), \quad \text{where } m > 0.$$

The pressure behavior is chiefly governed by the numerical values of the parameter m . For each category of fluids, we present the m vs. edge (singularity) angle dependence, and that for the two types of flows previously described. In particular, it is proved that, for corner angles for which the edge may be pictured as a hollow shaped cavity, the portion of the yield stress fluid entrapped in a region close to the tip—now located at the bottom of the cavity—does not yield during the flow, i.e. takes on a solid pattern.

2. The constitutive laws and flow equations

2.1. Constitutive laws

The generalized Newtonian fluid constitutive equation (mostly used for shear flows) is given by [8–10]:

$$\boldsymbol{\sigma} = f(\dot{\gamma}) \mathbf{A}_1 \quad (2.1)$$

where $\boldsymbol{\sigma}$ is the Cauchy extra-stress tensor, $\mathbf{A}_1 = \nabla \mathbf{u} + (\nabla \mathbf{u})^T$ is the (traceless) first Rivlin–Eriksen tensor, \mathbf{u} the velocity field, and $f(\dot{\gamma})$ stands for the shear rate dependent viscosity; the shear rate $\dot{\gamma}$ is defined as usually using the second invariant $II(\mathbf{A}_1)$ of the \mathbf{A}_1 tensor, that is:

$$\dot{\gamma}^2 = II(\mathbf{A}_1) := \frac{1}{2} \text{tr}(\mathbf{A}_1^2).$$

We now pause to recall several particular forms of the constitutive law (2.1) that will be studied in this work.

Example 2.1.

- (1) For the constant function $f(\dot{\gamma}) = \mu$ an ordinary Newtonian fluid is obtained.
- (2) The generalized Newtonian n -power law fluid (with $0 < n < 1$ for the shear thinning case) is obtained when:

$$f(\dot{\gamma}) = \mu \dot{\gamma}^{n-1}, \quad \mu, n > 0. \quad (2.2)$$

- (3) The generalized Newtonian fluid with Carreau–Yasuda viscosity law is given by:

$$f(\dot{\gamma}) = \mu_\infty + (\mu_0 - \mu_\infty) [1 + (\lambda \dot{\gamma})^a]^{(n-1)/a},$$

$$\mu_\infty, \mu_0, \lambda, n, a > 0. \quad (2.3)$$

- (4) The Herschel–Bulkley yield stress (or viscoplastic) fluid: following Huilgol [11], the Cauchy-extra stress tensor reads ($\mu, n > 0$):

$$\boldsymbol{\sigma} = \left(\mu \dot{\gamma}^{n-1} + \frac{\sigma_0}{\dot{\gamma}} \right) \mathbf{A}_1 \quad \text{if } II^{1/2}(\boldsymbol{\sigma}) > \sigma_0,$$

$$\mathbf{A}_1 = 0 \quad \text{if } II^{1/2}(\boldsymbol{\sigma}) \leq \sigma_0,$$

where σ_0 is the yield stress value (which depends on a given material microstructure), and $II(\boldsymbol{\sigma})$ is the second invariant of the Cauchy extra-stress tensor, which for a shear flow of an incompressible fluid (i.e. $\text{tr} \boldsymbol{\sigma} = 0$) is given by:

$$II(\boldsymbol{\sigma}) := \frac{1}{2} \text{tr}(\boldsymbol{\sigma}^2).$$

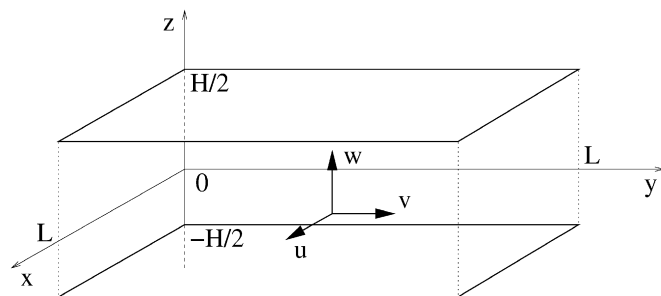


Fig. 1. The three-dimensional flow domain geometry (for details see text).

The particular case when $n = 1$ is known as the Bingham fluid. Another way to present the yield stress fluid is to make explicit $f(\dot{\gamma})$ (as in [8,12] or [13]):

$$f(\dot{\gamma}) = \begin{cases} \mu \dot{\gamma}^{n-1} + \frac{\sigma_0}{\dot{\gamma}} & \text{if } \dot{\gamma} \neq 0, \\ \text{solid behavior} & \text{if } \dot{\gamma} = 0. \end{cases} \quad (2.4)$$

As an aside, we point out that a thorough, rigorous mathematical presentation of general viscoplastic fluids is given in [14].

2.2. The thin film flow governing equations

The general form (i.e. for any three-dimensional domain—see Fig. 1) of the momentum balance equation and the incompressibility condition, are given respectively by:

$$\rho \left(\frac{\partial \mathbf{u}}{\partial t} + \mathbf{u} \cdot \nabla \mathbf{u} \right) = -\nabla p + \text{div} \boldsymbol{\sigma}, \quad (2.5)$$

$$\text{div} \mathbf{u} = 0, \quad (2.6)$$

where ρ is the (here constant) fluid density.

For the Hele–Shaw flows of interest to the present work (i.e. those confined between two narrowly gapped parallel plane surfaces), the fluid film thickness is negligible compared to the domain $x - y$ other dimensions. When this assumption is taken into account, a simplified form (more rigorously, an approximation) of Eqs. (2.5) and (2.6) is obtained.

Let the velocity field be $\mathbf{u} = (u, v, w)$, with its components functions of Cartesian coordinates (x, y, z) , and let the gap between the horizontal xOy plane and any of the two boundary planes be denoted $|z| = H/2$. As the flow is chiefly confined to the x and y directions, it is usually assumed (e.g. [3] and [5]) that w is negligible compared to u and v . Therefore, making use of the later assumption into Eqs. (2.5) and (2.6), one finds:

$$\frac{\partial p}{\partial x} = \frac{\partial}{\partial z} \left[f(\dot{\gamma}) \frac{\partial u}{\partial z} \right], \quad \frac{\partial p}{\partial y} = \frac{\partial}{\partial z} \left[f(\dot{\gamma}) \frac{\partial v}{\partial z} \right],$$

$$\frac{\partial p}{\partial z} = 0, \quad (2.7)$$

$$\frac{\partial u}{\partial x} + \frac{\partial v}{\partial y} + \frac{\partial w}{\partial z} = 0, \quad (2.8)$$

where:

$$\dot{\gamma} = \sqrt{\left(\frac{\partial u}{\partial z} \right)^2 + \left(\frac{\partial v}{\partial z} \right)^2}. \quad (2.9)$$

Remark 2.1. Eqs. (2.7) were obtained from Eqs. (2.5) above in a way similar to that described in [3], which is partially a heuristic one. In some recent papers [15–19] dealing with thin film flows of generalized Newtonian fluids, detailed proofs of their validity are given. They are based on the proof given by Bayada and Chambat in [20], for a common Newtonian fluid.

Regarding the boundary conditions, the no wall slip requires:

$$\mathbf{u} = 0 \quad \text{for } z = \pm \frac{H}{2}. \quad (2.10)$$

Given the flow domain symmetry, in the following we shall focus only on the upper half subdomain, i.e. the one for which $z = H/2$, and search for solutions restricted to $z \in [0, H/2]$ that satisfy:

$$\frac{\partial u}{\partial z} = \frac{\partial v}{\partial z} = 0 \quad \text{and} \quad w = 0 \quad \text{for } z = 0. \quad (2.11)$$

Remark 2.2. The equations (and the related considerations) presented so far hold true for domains with variable height also, i.e. those for which $H = H(x, y)$, and that without conflicting with the boundary conditions (2.11); as an example, we mention the flow domains for which $z = 0$ is a symmetry plane.

In the next section, we follow the procedure described in [3] which allows to eliminate the velocity field components from the momentum balance equation (2.7), and leads to a boundary value problem whose unique unknown is the pressure field.

2.3. The pressure equation

To achieve the forementioned goal, the first two equations of (2.7) are integrated with respect to z using the boundary conditions (2.11) to get:

$$z \frac{\partial p}{\partial x} = f(\dot{\gamma}) \frac{\partial u}{\partial z} \quad \text{and} \quad z \frac{\partial p}{\partial y} = f(\dot{\gamma}) \frac{\partial v}{\partial z}. \quad (2.12)$$

Next, squaring each equation in (2.12) and summing up side by side the results, give:

$$zX = f(\dot{\gamma})\dot{\gamma} \quad \text{where } X = \sqrt{\left(\frac{\partial p}{\partial x}\right)^2 + \left(\frac{\partial p}{\partial y}\right)^2}. \quad (2.13)$$

Let us assume there exists a function G such that:

$$f(\dot{\gamma})\dot{\gamma} = zX \iff \dot{\gamma} = G(zX). \quad (2.14)$$

Remark 2.3. This assumption is tantamount to saying the equation $\dot{\gamma} f(\dot{\gamma}) = zX$ is explicitly solvable in terms of $\dot{\gamma}$, which of course triggers restrictions on the $f(\dot{\gamma})$ algebraic form. In this work we shall first focus on particular cases where Eq. (2.14) does have an explicit solution $\dot{\gamma} = G(zX)$ and exemplify using well-known viscosity relationships. However, situations where an explicit solution is not obtainable are not ruled out. In fact, it will be proved that, insofar as the pressure field map around the edge is the main concern, what matters mostly (and influences it) is the fluid asymptotic behavior for low ($\dot{\gamma} \rightarrow 0$) and high ($\dot{\gamma} \rightarrow +\infty$) shear rates; see Section 3.3 for details.

Example 2.2. For the Herschel–Bulkley fluid, $G(zX)$ is taken as a particular case of Eq. (2.14), i.e.:

$$G(zX) = \begin{cases} \left(\frac{zX - \sigma_0}{\mu}\right)^{1/n} & \text{if } zX > \sigma_0, \\ 0 & \text{if } zX \leq \sigma_0. \end{cases} \quad (2.15)$$

Eq. (2.15) above takes into account the fact that the yield stress fluid moves as a solid for $zX \leq \sigma_0$.

Next, making use of Eqs. (2.12) and (2.13) and the definition of G (see Eq. (2.14) above), we obtain:

$$\frac{\partial u}{\partial z} = \frac{G(zX)}{X} \frac{\partial p}{\partial x} \quad \text{and} \quad \frac{\partial v}{\partial z} = \frac{G(zX)}{X} \frac{\partial p}{\partial y}. \quad (2.16)$$

Using the method described in [21], we proceed as following: Eqs. (2.16) right above are twice integrated, and after use of boundary conditions Eq. (2.10) is made, one gets:

$$u(x, y, z) = \int_{H/2}^z \frac{\partial u}{\partial z}(x, y, t) dt = \frac{1}{X} \left(\int_{H/2}^z G(tX) dt \right) \frac{\partial p}{\partial x}, \quad (2.17)$$

$$v(x, y, z) = \int_{H/2}^z \frac{\partial v}{\partial z}(x, y, t) dt = \frac{1}{X} \left(\int_{H/2}^z G(tX) dt \right) \frac{\partial p}{\partial y}. \quad (2.18)$$

Consequently, the flow fluxes q_u and q_v can now be written as:

$$q_u(x, y) = 2 \int_0^{H/2} u(x, y, z) dz = \frac{2}{X} \left(\int_0^{H/2} zG(zX) dz \right) \frac{\partial p}{\partial x}, \quad (2.19)$$

$$q_v(x, y) = 2 \int_0^{H/2} v(x, y, z) dz = \frac{2}{X} \left(\int_0^{H/2} zG(zX) dz \right) \frac{\partial p}{\partial y}. \quad (2.20)$$

Finally, using the incompressibility restriction Eq. (2.7) together with the boundary conditions Eqs. (2.10) and (2.11), we find that:

$$\frac{\partial q_u}{\partial x} + \frac{\partial q_v}{\partial y} = 0. \quad (2.21)$$

Eq. (2.21) can be rewritten in operator form as $\text{div}(g(X)\nabla p) = 0$, or, more conveniently for further calculations, as:

$$\frac{\partial}{\partial x} \left[g(X) \frac{\partial p}{\partial x} \right] + \frac{\partial}{\partial y} \left[g(X) \frac{\partial p}{\partial y} \right] = 0 \quad \text{with} \\ X = \sqrt{\left(\frac{\partial p}{\partial x}\right)^2 + \left(\frac{\partial p}{\partial y}\right)^2} \quad (2.22)$$

where the function g is:

$$g(X) = \frac{2}{X} \left(\int_0^{H/2} zG(zX) dz \right). \quad (2.23)$$

Remark 2.4. For sake of clarity we now pause to exemplify how the above presented formalism applies to a Newtonian fluid, i.e. for which $f(\dot{\gamma}) = \mu$. In this case, $G(zX) = zX/\mu$ (see Eq. (2.14)). Therefore, $g(X) = H^3/12\mu$ (see Eq. (2.23)) and Eq. (2.22) becomes the well-known Reynolds equation:

$$\text{div} \left(\frac{H^3}{12\mu} \nabla p \right) = 0.$$

2.4. Remarks on antisymmetric half plane solution

In this section we explore the behavior of nontrivial antisymmetric solutions $p(x, y)$ to Eq. (2.22) defined over the half plane $\{(x, y) \in \mathbb{R}^2, x > 0\}$ (see Fig. 2) such that $p(x, 0) = 0$; full solution details are given in the next section.

Assume one searches for a solution p independent of the variable x while solving:

$$\left[g(|p'(y)|) p'(y) \right]' = 0 \quad \text{for } y \in \mathbb{R}, \\ p(0) = 0.$$

Whenever the mapping $X \mapsto Xg(X)$ is strictly monotonic (either increasing or decreasing), there exists a unique nonzero solution (up to an integration constant which can be calculated by setting $p'(0) = 1$ for example). Such a solution is given by:

$$p(x, y) = y.$$

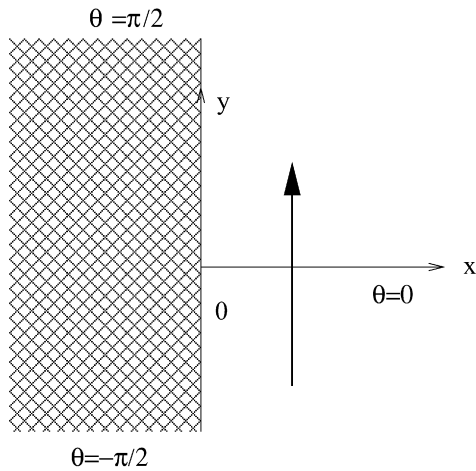


Fig. 2. The half-plane domain (for details see text).

It will next be readily perceived that Newtonian, power law and Carreau–Yasuda fluids are compatible with the forementioned strict monotonicity restriction. However, the yield stress fluid case is different: the mapping $x \mapsto xg(x)$ vanishes for $x \leq \sigma_0$ and is monotonic for $x > \sigma_0$, where σ_0 denotes the yield stress value. Actually one gets:

solid-like behavior if $p'(0) \leq \sigma_0$,

$p(x, y) = p'(0)y$ if $p'(0) > \sigma_0$.

The yield stress fluid case is studied in Section 3.4.

3. Corner edge solution

Let us now search for solutions to Eq. (2.22) that are valid in the region neighboring the edge (singularity) peak. The tip angle is assumed fixed in time and equal to 2α (see Fig. 3).

To do so, Eq. (2.22) is expressed in polar coordinates (r, θ) , the axes of which are centered at the forementioned singularity:

$$\frac{\partial}{\partial r} \left[rg(X) \frac{\partial p}{\partial r} \right] + \frac{1}{r} \frac{\partial}{\partial \theta} \left[g(X) \frac{\partial p}{\partial \theta} \right] = 0, \quad (3.1)$$

for $(r, \theta) \in \mathbb{R}_+^* \times]-\alpha, \alpha[$, where $\alpha \in]0, \pi[$ and

$$X = \sqrt{\left(\frac{\partial p}{\partial r}\right)^2 + \frac{1}{r^2} \left(\frac{\partial p}{\partial \theta}\right)^2}. \quad (3.2)$$

3.1. Pressure behavior close to the geometric singularity

We now turn our attention to finding particular solutions to Eq. (2.22). To achieve this, we assume for the pressure field an asymptotic expansion representation of the form:

$$p(r, \theta) = r^m \varphi(\theta) + o(r^m), \quad m > 0. \quad (3.3)$$

Searching for this type of solutions while dealing with stress behavior near geometric singularities is not unusual. In passing, we mention that Moffatt [1], and later on Hassager and Lauridsen [3], have also searched for the same type of solution in their quest to solve flow problems around sharp edges. Moreover, the stress behavior close to sharp crystal edges in polycrystalline materials under large deformations is also modelled using an asymptotic expansion of the same type as the one used here: see for example the recent work by Picu and Gupta [22,23].

When Eq. (3.3) is introduced into Eq. (3.2), after retaining only the dominant term, leads to:

$$X = r^{m-1} \sqrt{m^2 \varphi(\theta)^2 + \varphi'(\theta)^2}. \quad (3.4)$$

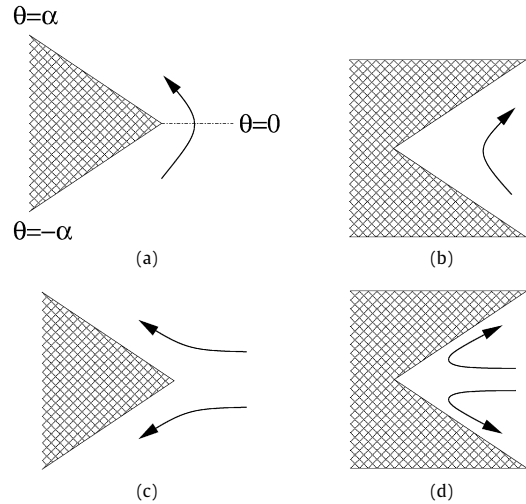


Fig. 3. The flows under scrutiny take place in a region close to the edge tip. The arrows on the first two drawings show the direction of antisymmetric flows, while on the last two they indicate the direction of symmetric flows. Sketches (b) and (d) correspond to the case where the edge angle value is chosen so that the sharp edge becomes a hollow shaped cavity.

Next, making use of the dominant (i.e. of the m th-rank) term in the expansion Eq. (3.3) into Eq. (3.1) gives:

$$\frac{\partial}{\partial \theta} \left[g(X) \frac{\partial \varphi}{\partial \theta} \right] + m[mg(X) + (m-1)Xg'(X)]\varphi = 0. \quad (3.5)$$

The above equation will be solved for φ with respect to two types of boundary conditions, each of which being related to a particular flow. For the antisymmetric flows (see Figs. 3(a) and 3(b)), the boundary conditions are (see also [3]):

$$\varphi'(\alpha) = 0 \quad \text{and} \quad \varphi(0) = 0, \quad \text{for antisymmetric flow.} \quad (3.6)$$

For symmetric flows (see Figs. 3(c) and 3(d)) the boundary conditions look:

$$\varphi'(\alpha) = 0 \quad \text{and} \quad \varphi'(0) = 0, \quad \text{for symmetric flow.} \quad (3.7)$$

The problem with antisymmetric boundary conditions will be addressed first (in the next section), followed by that with symmetric boundary conditions (in Section 3.5).

3.2. Newtonian and power-law fluids

3.2.1. Newtonian fluid case

For a Newtonian fluid, $f(\dot{\gamma}) = \mu$ (see in Example 2.1). The functions G and g are obtained explicitly using Eqs. (2.14) and (2.23) (as mentioned in Remark 2.4). Therefore, in this case $g(X) = H^3/(12\mu)$ is the constant function, and the particular form of the pressure differential equation Eq. (3.5) and the antisymmetric boundary conditions Eq. (3.6) read:

$$\varphi'' + m^2 \varphi = 0, \quad \varphi(0) = 0 \quad \text{and} \quad \varphi'(\alpha) = 0.$$

In the above, m^2 is the first nonzero eigenvalue of the Laplacian solved with respect to the boundary conditions Eq. (3.6). Moreover, (see also Fig. 6 in Section 3.3):

$$m = \frac{\pi}{2\alpha},$$

eigenvalue to which corresponds the eigenfunction $\varphi(\theta) = \sin[\pi\theta/(2\alpha)]$.

3.2.2. Power-law fluid case

For generalized n -power Newtonian fluids (see Eq. (2.2)), carrying out calculations in a way similar to the one given right above leads to:

$$f(\dot{\gamma}) = \mu \dot{\gamma}^{n-1}$$

which, using Eq. (2.14), gives further:

$$G(zX) = \left(\frac{zX}{\mu}\right)^{1/n}. \tag{3.8}$$

From above we obtain for the function g (defined in Eq. (2.23)) the following expression:

$$\begin{aligned} g(X) &= \frac{2}{X} \int_0^{H/2} zG(zX) dz \\ &= \frac{2X^{1/n-1}}{\mu^{1/n}} \int_0^{H/2} z^{1/n+1} dz \\ &= \frac{H^{1/n+2}}{\mu^{1/n}(1/n+2)2^{1/n+1}} X^{1/n-1}. \end{aligned}$$

Therefore $g(X) = \text{const } X^{1/n-1}$.

We are now in a position that enables us to relate our results to those of Aronsson and Janfalk. Indeed, Theorem 3.1.6 in [5, p. 353], states that, for power-law fluids for which $g(X) = \text{const } X^{1/n-1}$ and for any angle $\alpha \in]0, \pi[$, $\alpha \neq \pi/2$, there exists (up to a multiplicative constant) a unique function φ and a real number $m > 0$ which is a solution of Eq. (3.5) and of Eq. (3.6); moreover $\varphi' > 0$ on $]-\alpha, \alpha[$. The pressure field can now be computed by solving the following boundary value problem (which is a particular case of Eq. (3.5)):

$$\begin{cases} \varphi'' + m^2\varphi + \left(\frac{1}{n} - 1\right)m(m-1)\frac{\varphi'^2 + m^2\varphi^2}{(1/n)\varphi'^2 + m^2\varphi^2}\varphi = 0, \\ \varphi'(\alpha) = 0, \quad \text{and} \quad \varphi(0) = 0. \end{cases} \tag{3.9}$$

Eq. (3.9) is solved numerically using a fast convergent algorithm based on the “shooting” technique. The solution is denoted:

$$\varphi = \Phi_\alpha(\theta). \tag{3.10}$$

The numerical values of m computed here are identical to those reported in [3]. Next, on Fig. 4 we show the shape of successive iterations that converge towards the final solution $\Phi_\alpha(\theta)$. As $p(r, \theta) = r^m \varphi(\theta)$ has now been obtained, for convenience (and sake of clarity) it may be next expressed in Cartesian coordinates also centered at the edge tip. This is done on Fig. 5, where $p(x, y)$ is plotted for $n = 0.1$, $\alpha = 3\pi/4$, chosen arbitrarily to exemplify.

Moreover, Theorem 3.2.4 in [5, p. 359], gives m explicitly; with this work notations, the result is:

$$m = \frac{\beta(\alpha) + n - 1}{\beta(\alpha) - 1} := M_\alpha, \tag{3.11}$$

where:

$$\begin{aligned} \beta(\alpha) &= \frac{1}{2} \left(1 - n \pm \sqrt{(n-1)^2 + 4\delta^2 n} \right) \quad \text{and} \\ \delta &= \frac{\pi}{|\pi - 2\alpha|}. \end{aligned} \tag{3.12}$$

Remark 3.1. This work power m given in Eq. (3.11), and function β presented in Eq. (3.12) right above, do correspond to l and β_1 given in Eq. (4.4) in [5, p. 362].

In the above equation that defines β , the sign is set equal to $+$ if $2\alpha < \pi$ and equal to $-$ if $2\alpha > \pi$. The relationship m vs. edge angle α is plotted in Fig. 6 (with $n = 0.5$ chosen as an example).

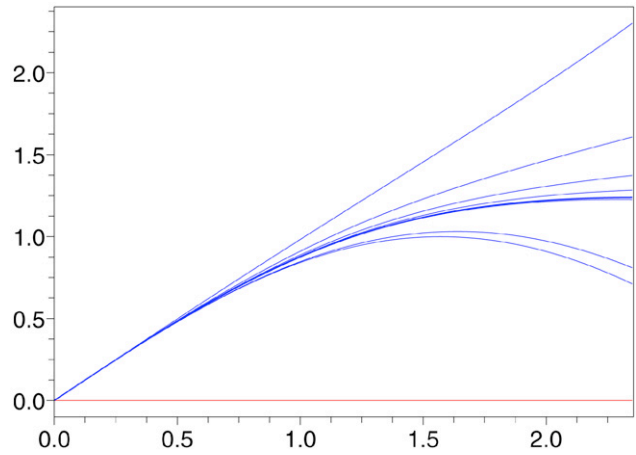


Fig. 4. Successive numerical iterations that converge towards the solution $\varphi = \Phi_\alpha(\theta)$ of Eq. (3.9).

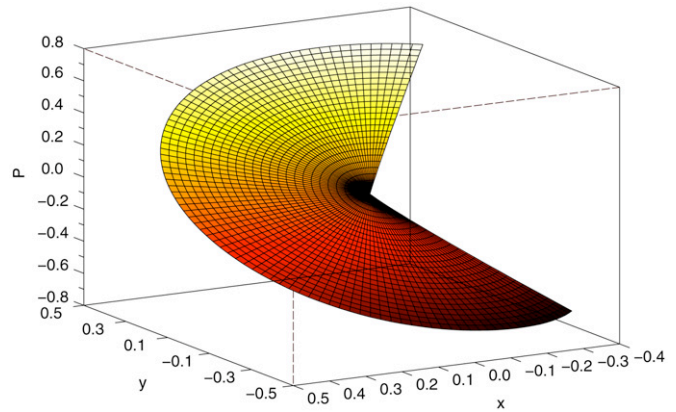


Fig. 5. The pressure field $p = p(x, y)$ in Cartesian coordinates, solution of the power-law antisymmetric flow boundary value problem. Here $n = 0.1$ and $\alpha = 3\pi/4$ were chosen arbitrarily to exemplify.

Next we recall here that for $2\alpha = \pi$ one gets the half plane domain case that was studied in Section 2.4 above; there it was found that the pressure field has the form $p(x, y) = y$ in Cartesians, that is $p(r, \theta) = r^1 \sin\theta$ in polar coordinates, and that $M_{\pi/2} = 1$.

Eventually one has:

Proposition 3.1. Let an n -power fluid antisymmetric flow take place in a sharp edge neighborhood of angle $\alpha \in]0, \pi[$. Then the pressure field may be expressed as $p(r, \theta) = r^m \varphi(\theta)$, where

$$m = M_\alpha, \quad \text{see Eq. (3.11),}$$

$$\varphi = \Phi_\alpha, \quad \text{see Eq. (3.10).}$$

Remark 3.2. Note that the case $2\alpha = \pi$ is recovered when the monotonicity of m vs. α relationship is used. Indeed, given that in Theorem 3.1.6 in [5] it is shown that m is a decreasing function of α , it follows that:

$$\alpha < \pi/2 \implies M_\alpha > 1,$$

$$\alpha > \pi/2 \implies M_\alpha < 1. \tag{3.13}$$

Remark 3.3. As the reason behind the fact that $\varphi' > 0$ may not be readily perceived at a first glance, the present remark is devoted to shed more light on it. If it is not required that $\varphi' > 0$, then

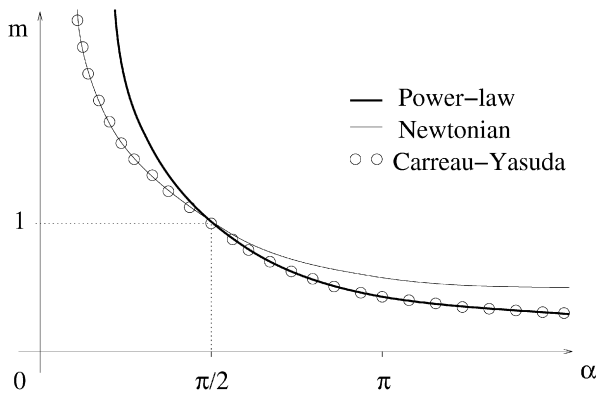


Fig. 6. The exponent m vs. edge angle α dependence for a Newtonian fluid (thin curve), power law fluid (thick curve), and Carreau–Yasuda fluid (open symbols); for the last two fluids we set $n = 0.5$ to exemplify.

the solution to the boundary value problem given in Eqs. (3.5)–(3.6) is not unique. Indeed, if φ' vanishes for any $\tilde{\alpha} \in]-\alpha, \alpha[$, then one may construct other solutions defined over any subintervals $]-\alpha, \tilde{\alpha}[$ and $]\tilde{\alpha}, \alpha[$ with nonzero first order derivatives. In the later case, since the $m = m(\alpha)$ function is decreasing, the values of m obtained for such a solution exceed those obtained for (edge angle) α . Therefore, only the least $m > 0$ value leads to the solution φ which is such that $\varphi' > 0$. Moreover, if $\varphi' = 0$, then compliance with antisymmetric flow boundary condition $\varphi(0) = 0$ results in the solution $\varphi = 0$, which is of no physical interest.

3.3. The Carreau–Yasuda fluid case

3.3.1. Generalities

As the flows around sharp edges of more complex generalized Newtonian fluids such as the Carreau–Yasuda ones have not previously been studied, this part of the Letter is devoted to it.

On the one hand, note that viscosity functions $f(\dot{\gamma})$ more complex than the power law one will exhibit different asymptotic behaviors for low and high shear rates $\dot{\gamma}$. Formally, let $f(\dot{\gamma})$ be asymptotically equivalent to $\dot{\gamma}^{a_0}$ ($\dot{\gamma}^{a_\infty}$) for small (large) $\dot{\gamma}$ values. This implies that the corresponding function g (defined in Eq. (2.23)) behaves asymptotically as:

$$g(X) \underset{X \rightarrow 0}{\sim} C_0 X^{b_0},$$

$$g(X) \underset{X \rightarrow \infty}{\sim} C_\infty X^{b_\infty}.$$

On the other hand, of interest here is the function $X(r, \theta)$ behavior close to the singularity tip (i.e. whenever r shrinks down to 0), behavior on which depends that of $g(X)$. The forementioned pattern is strongly influenced by the m values. Indeed, if $m > 1$, then $\lim_{r \rightarrow 0} X(r, \theta) = 0$, where $X(r, \theta)$ is given in Eq. (3.4). In this case:

$$g(X(r, \theta)) \underset{r \rightarrow 0}{\sim} C_0 [X(r, \theta)]^{b_0}$$

and the pressure Eq. (3.5) is to be solved for X^{b_0} . If $m < 1$, then $\lim_{r \rightarrow 0} X(r, \theta) = +\infty$, g behaves asymptotically as:

$$g(X(r, \theta)) \underset{r \rightarrow \infty}{\sim} C_\infty [X(r, \theta)]^{b_\infty}$$

and the pressure equation is to be solved for X^{b_∞} . Finally, the case $m = 1$ corresponds to angle values $\alpha = \pi/2$ (as seen in Section 2.4).

One particular difficulty consists in that one does not know beforehand the values of m , i.e. whether $m \lesseqgtr 1$. Nevertheless, in the upcoming sections, we shall rigorously prove for the Carreau–Yasuda fluid and for the yield stress Herschel–Bulkley one that it is possible, first, to calculate the values of m , and second, evaluate φ .

3.3.2. Application to the Carreau–Yasuda fluid model

For a Carreau–Yasuda viscosity law (see Eq. (2.3)) one has:

$$f(\dot{\gamma}) \sim \mu_0 \quad \text{at } 0,$$

$$f(\dot{\gamma}) \sim C \dot{\gamma}^{n-1} \quad \text{at } +\infty.$$

This is a particular case of the one addressed in the previous section, as to $b_0 = 0$ corresponds the Newtonian case (see Section 3.2.1), and to $b_\infty = 1/n - 1$ the power-law case (see Section 3.2.2).

Next:

- if the edge angle α is such that $2\alpha < \pi$, then m cannot be less than 1, because $m < 1$ leads to a power law pattern of exponent b_∞ which is incompatible with Eq. (3.13). Also, the case $m = 1$ is to be avoided as it corresponds to $2\alpha = \pi$ (see Section 2.4). Therefore $m > 1$. Close to the singularity, the fluid exhibits a purely Newtonian pattern ($b_0 = 0$; see also Section 3.2.1). Moreover:

$$m = \frac{\pi}{2\alpha} \quad \text{and} \quad \varphi(\theta) = \sin[\pi\theta/(2\alpha)].$$

- Proceeding as in the proof given right above, one can show that if $2\alpha > \pi$, then $m < 1$. We eventually get:

$$m = M_\alpha \quad \text{and} \quad \varphi = \Phi_\alpha(\theta),$$

where $\Phi_\alpha(\theta)$ above is that of Eq. (3.10). The above observations are formally summarized below.

Proposition 3.2. Given an antisymmetric flow of a Carreau–Yasuda fluid (Eq. (2.3)) that takes place in a neighborhood of a sharp edge of angle $\alpha \in]0, \pi[$, then the pressure field may be expressed as $p(r, \theta) = r^m \varphi(\theta)$, where:

$$\varphi(\theta) = \begin{cases} \sin[\pi\theta/(2\alpha)] & \text{if } \alpha \leq \pi/2, \\ \Phi_\alpha(\theta) & \text{if } \alpha > \pi/2. \end{cases}$$

and

$$m = \begin{cases} \frac{\pi}{2\alpha} & \text{if } \alpha \leq \pi/2, \\ M_\alpha & \text{if } \alpha > \pi/2, \end{cases}$$

where the functions Φ_α and M_α are defined, respectively, in Eq. (3.10) and in Eq. (3.11) above.

Next, the $m = m(\alpha)$ functions corresponding to Newtonian, power-law and Carreau–Yasuda fluids are given on Fig. 6.

3.4. The yield stress fluids: Antisymmetrical flows case

The yield stress fluid case needs particular care as the function $f = f(\dot{\gamma})$ has no indisputable mathematical meaning for 0 argument. However, based on previous Example 2.2, one may define the function G as:

$$G(zX) = \begin{cases} \left(\frac{zX - \sigma_0}{\mu}\right)^{1/n} & \text{if } zX > \sigma_0, \\ 0 & \text{if } zX \leq \sigma_0. \end{cases} \quad (3.14)$$

Moreover, as the Herschel–Bulkley continuum moves like a solid within the domain for which $\sigma_0/X > H/2$, it follows that $g(X) = 0$ (where g is defined in Eq. (2.23)). Outside this domain, the function g is given by:

$$g(X) = \frac{2}{\mu^{1/n} X} \int_{\sigma_0/X}^{H/2} z(zX - \sigma_0)^{1/n} dz \quad (3.15)$$

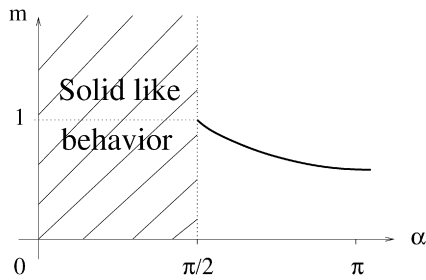


Fig. 7. Antisymmetrical flow case: m vs. (singularity angle) α dependence for Herschel–Bulkley yield stress fluids.

and after carrying out the integration one gets explicitly:

$$g(X) = \begin{cases} \frac{2n}{\mu^{1/n} X^3} \left[\frac{(HX/2 - \sigma_0)^{(2n+1)/n}}{2n+1} + \sigma_0 \frac{(HX/2 - \sigma_0)^{(n+1)/n}}{n+1} \right] & \text{if } X > \frac{2\sigma_0}{H}, \\ 0 & \text{if } X \leq \frac{2\sigma_0}{H}. \end{cases}$$

When $X \rightarrow +\infty$, $g(X)$ has the following asymptotic pattern:

$$g(X) \underset{X \rightarrow +\infty}{\sim} C X^{1/n-1} \tag{3.16}$$

where C is a nonzero real constant, and $b_\infty = 1/n - 1$.

A solid-like behavior is obtained for $m > 1$ (since $X(r, \theta)$ tends to 0 as r tends to 0), while for $m < 1$ the continuum body exhibits a power law fluid behavior. Specifically, by a reasoning similar to that in the precedent section, one shows that (see also Fig. 7):

Proposition 3.3. *Given an antisymmetric flow of a Herschel–Bulkley (yield stress) fluid that takes place in a neighborhood of an edge of angle $\alpha \in]0, \pi[$, then:*

- for $2\alpha < \pi$, the fluid exhibits a solid-like behavior,
- for $2\alpha > \pi$, the pressure field is given by $p(r, \theta) = r^m \varphi(\theta)$, where $m = M_\alpha$, and $\varphi(\theta) = \Phi_\alpha(\theta)$. M_α and Φ_α are actually those obtained in Section 3.2—and are recalled below for convenience:

$$m = M_\alpha = \frac{\beta(\alpha) + n - 1}{\beta(\alpha) - 1}, \tag{3.17}$$

where:

$$\beta(\alpha) = \frac{1}{2} \left[1 - n \pm \sqrt{(n-1)^2 + 4\delta^2 n} \right] \quad \text{and} \quad \delta = \frac{\pi}{|\pi - 2\alpha|},$$

Φ_α is to be obtained numerically, as in Section 3.2.

3.5. Symmetric flows case

This section methodology for solving the problem of symmetrical flows of generalized Newtonian and yield stress fluids is similar in spirit to the one for antisymmetrical flows in the precedent sections. First, we deal with the issue of finding the pressure field for power law fluids, followed by results for more general fluids. As the subsequent calculations are similar in nature to those of previous sections (which addressed the problem of antisymmetric flows), we do not present all calculation details. However the peculiarities of symmetrical flows are made bold. Moreover, the results will be presented in terms of M_α and Φ_α .

We search for solutions $p(r, \theta) = r^m \varphi(\theta) + o(r^m)$, $m > 0$ to Eq. (2.22). In doing so, the least m value is computed numerically. The relationship between φ and m is given by Eq. (3.5). The difference with respect to the antisymmetric flow case lays on the prescribed boundary conditions (compare Eq. (3.6) vs. Eq. (3.7)).

Next, for a Newtonian fluid symmetric flow, the function φ and power $m > 0$ must satisfy $\varphi'' + m^2 \varphi = 0$, $\varphi'(0) = 0$, $\varphi'(\alpha) = 0$. The least $m > 0$ value for which this equation has a nontrivial solution is $m = \pi/\alpha$, to which corresponds $\varphi(\theta) = \sin[\pi\theta/\alpha]$.

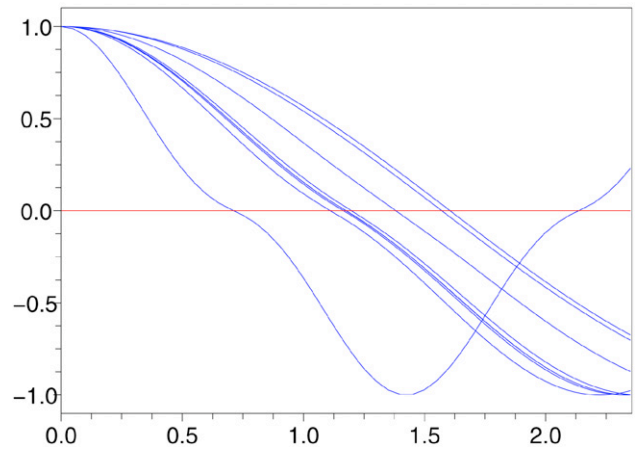


Fig. 8. Successive numerical iterations that converge towards the solution $\varphi = \Phi_{\alpha/2}$, where $\alpha = 3\pi/4$ and $n = 10$ have been arbitrarily chosen to exemplify.

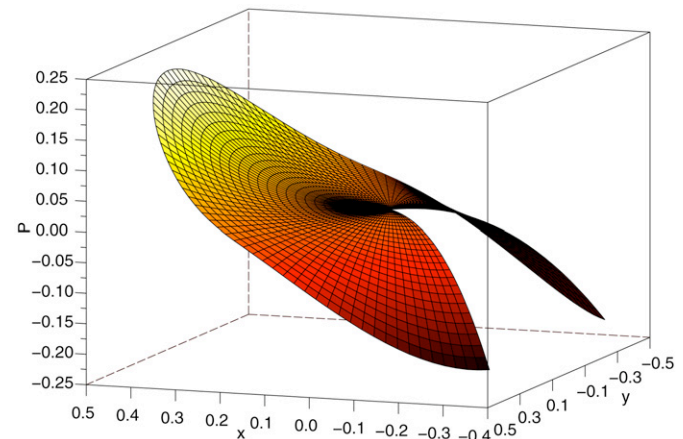


Fig. 9. The pressure field $p(x, y)$ in Cartesian coordinates, where $\alpha = 3\pi/4$ and $n = 10$ have been arbitrarily chosen to exemplify.

3.5.1. Power-law fluid case

A solution $p(r, \theta) = r^m \varphi(\theta)$ valid for a symmetrical flow around a sharp edge must satisfy $\varphi'(0) = 0$ and $\varphi'(\alpha) = 0$ (see the boundary conditions in Eq. (3.7) and Fig. 3(c) and Fig. 3(d)). These specific boundary conditions lead to considering two types of solutions to Eq. (3.5):

- solutions for which $\varphi'(\theta)$ vanishes only for $\theta \in \{0, \pm\alpha\}$; in this case the least $m > 0$ value is $m = M_{\alpha/2}$ (with $M_{\alpha/2}$ given by Eq. (3.17); see also Remark 3.3) and $\varphi = \Phi_{\alpha/2}$.
- solutions for which $\varphi' \equiv 0$, which in turn triggers $m = 1 - n$ to ensure compatibility with Eq. (3.5) and that $\varphi = 1$.

Let us remember the goal is to find a solution φ to the boundary value problem Eq. (3.5) and Eq. (3.7) that corresponds to the least positive m value. Given that $M_{\alpha/2} > 1$ for any angle $\alpha \in]0, \pi[$ and that $1 - n < 1$ in the shear thinning case, one readily obtains the following:

Proposition 3.4. *Let an n -power fluid symmetric flow take place in a sharp edge neighborhood of angle $\alpha \in]0, \pi[$. Then the pressure field may be expressed as $p(r, \theta) = r^m \varphi(\theta)$, where:*

$$m = \begin{cases} 1 - n & \text{if } 0 < n < 1 \text{ (shear thinning pattern),} \\ M_{\alpha/2} & \text{if } n \geq 1 \text{ (shear thickening pattern).} \end{cases}$$

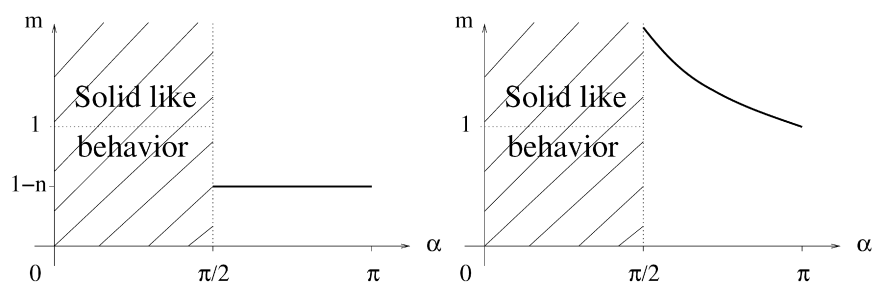


Fig. 10. The m vs (edge angle) α dependence for a Herschel–Bulkley fluid (as defined in Eq. (2.4) in Section 2.1). On the left $n = 0.5$ and the fluid is shear thinning; on the right $n = 2$ and the fluid is shear thickening; the values of n were chosen arbitrarily to exemplify.

M above is that of Eq. (3.17), and

$$\varphi(\theta) = \begin{cases} 1 & \text{if } 0 < n < 1, \\ \Phi_{\alpha/2} & \text{if } n \geq 1. \end{cases} \quad (3.18)$$

As an aside, one observes that Proposition 3.4 is this section counterpart of Proposition 3.1 that concerns antisymmetric flows.

We present on Fig. 8 the iterations converging towards the solution $\varphi = \Phi_{\alpha/2}$, and on Fig. 9 the pressure field in Cartesian coordinates.

3.5.2. General case

The precedent section theoretical framework can be used to study the flows around geometrical singularities for more complex fluids. Following along the lines of previous sections that dealt with antisymmetrical flows, one sees that what matters most is the constitutive equation limiting behavior for low and high shear rates.

Specifically, for a fluid whose shear rate dependent viscosity exhibits the following asymptotic patterns:

$$f(\dot{\gamma}) \underset{\dot{\gamma} \rightarrow 0}{\sim} C_0 \dot{\gamma}^{a_0},$$

$$f(\dot{\gamma}) \underset{\dot{\gamma} \rightarrow \infty}{\sim} C_\infty \dot{\gamma}^{a_\infty},$$

its behavior will be similar to that of a fluid for which either $f(\dot{\gamma}) = \dot{\gamma}^{a_0}$ (whenever $\alpha < \pi/2$) or $f(\dot{\gamma}) = \dot{\gamma}^{a_\infty}$ (whenever $\alpha > \pi/2$). The $m = m(\alpha)$ dependence is fully determined by results obtained for power law fluids. Moreover, a Herschel–Bulkley fluid will behave solid-like whenever the edge angle is small enough, i.e. $\alpha < \pi/2$. To exemplify, we present on Fig. 10 the $m = m(\alpha)$ function for a yield stress fluid in two situations: when $n = 0.5$ (shear thinning behavior) and when $n = 2$ (shear thickening behavior), where the n values were chosen arbitrarily.

4. Conclusions

In this Letter we report several new results regarding the flows around sharp edges (modelled as geometric singularities) of several generalized Newtonian and Herschel–Bulkley and Bingham yield stress fluids. Two types of flows are under scrutiny: antisymmetrical (i.e. perpendicular to the edge symmetry axis) and symmetrical (i.e. parallel to the singularity symmetry axis and directed towards the sharp edge tip).

The main aim is to obtain the edge angle α influence upon the pressure field p . For convenience, p is expressed in a polar coordinate system centered at the edge tip. Next, p is assumed to have an asymptotic expansion the terms of which consist of products of two factors: one depends on the polar radius r and the other on the polar angle θ . Regarding this later assumption, there is agreement among various authors that the pressure field has to be of the form used in this work: see for example [3] and/or [22,23] and references cited therein. Next, we have set up a general framework within which knowledge of the explicit viscosity dependence upon

shear rate $\dot{\gamma}$ law is not necessary to obtain the pressure field in an edge neighborhood.

For antisymmetrical flows, the influence of edge angle α upon $p(r, \theta)$ is studied numerically. For the particular case of power law fluids, excellent agreement is obtained with the results previously published in [3] and [5]. Next, we computed the pressure field $p(r, \theta)$ for Carreau–Yasuda and Herschel–Bulkley yield stress fluids—cases not previously studied. For yield stress fluids, our results show that:

- for edge angles in excess of $\pi/2$ (i.e. flows over the edge tip, see Fig. 3(a)) the material does yield and behaves liquid-like;
- for edge angles less than $\pi/2$ (in which case the flow is such that parts of the material are trapped inside a sharp cavity; see Fig. 3(b)), close to the singularity tip the fluid does not yield and behaves solid-like;

The symmetrical flow around singularity, an issue not previously addressed—save for the power law viscosity in [3]—is studied within our general framework. The pressure p dependence upon angle α is obtained for both quasi-Newtonian and Bingham fluids in a manner similar to the antisymmetrical flow case.

Acknowledgements

L.I.P. is indebted to Professor Raja R. Huilgol, Flinders University of South Australia, for a four months sabbatical invitation, a stay during which parts of this work were addressed. Both authors gratefully acknowledge Professor Raja R. Huilgol and the Anonymous Referee for helpful comments.

References

- [1] H.K. Moffatt, J. Fluid Mech. 18 (1963) 1.
- [2] C.A. Hieber, S.F. Shen, J. Non-Newtonian Fluid Mech. 7 (1980) 1.
- [3] O. Hassager, T.L. Lauridsen, J. Non-Newtonian Fluid Mech. 29 (1988) 337.
- [4] R.R. Huilgol, R.I. Tanner, J. Non-Newtonian Fluid Mech. 2 (1977) 89.
- [5] G. Aronsson, U. Janfalk, Eur. J. Appl. Math. 3 (1992) 343.
- [6] R.R. Huilgol, J. Non-Newtonian Fluid Mech. 138 (2006) 209.
- [7] L. Kondic, P. Palffy-Muhoray, M. Shelley, Phys. Rev. E 54 (1996) R4536.
- [8] R. Byron-Bird, R.C. Armstrong, O. Hassager, Dynamics of Polymeric Liquids, second ed., Fluid Mechanics, vol. 1, Wiley & Sons, 1987.
- [9] R.R. Huilgol, N. Phan-Thien, Fluid Mechanics of Viscoelasticity, Elsevier, 1997.
- [10] F.A. Morrison, Understanding Rheology, Oxford Univ. Press, 2001.
- [11] R.R. Huilgol, Phys. Fluids 14 (2002) 1269.
- [12] R. Byron-Bird, G.C. Day, B.J. Yarusso, Rev. Chem. Eng. 1 (1982) 1.
- [13] N. Roquet, P. Saramito, Comput. Methods Appl. Mech. Engrg. 192 (2003) 3317.
- [14] I.R. Ionescu, M. Sofonea, Functional and Numerical Methods in Viscoplasticity, Oxford Mathematical Monographs, Oxford Univ. Press, 1993.
- [15] F. Boughanim, R. Tapiéro, Appl. Anal. 57 (1995) 243.
- [16] K. Taous, C. R. Acad. Sci. Paris Sér. I: Math. 323 (1996) 1213.
- [17] R. Bunoiu, S. Kesavan, J. Math. Anal. Appl. 293 (2004) 405.
- [18] M. Boukrouche, R. El Mir, Nonlinear Anal. 59 (2004) 85.
- [19] J.-M. Sac-Épée, K. Taous, Asymptot. Anal. 44 (2005) 151.
- [20] G. Bayada, M. Chabhat, Appl. Math. Optim. 14 (1986) 73.
- [21] A. Bergwall, Quart. Appl. Math. 60 (1) (2002) 37.
- [22] C.R. Picu, V. Gupta, Int. J. Solids Structures 33 (1996) 1535.
- [23] C.R. Picu, V. Gupta, J. Mech. Phys. Solids 45 (1997) 1495.